Optimizing the Curie temperature of pseudo-binary $R_xR'_{2-x}Fe_{17}$ (R, R' = rare earth) for magnetic refrigeration

Pablo Álvarez-Alonso[1,*], Pedro Gorria[2], Gabriel Cuello[3], Inés Puente Orench[3,4], José L. Sánchez Llamazares[5], Victorino Franco[6], Marian Reiffers[7] and Jesús A. Blanco[8].

[1]Departamento de Electricidad y Electrónica, UPV/EHU, Bº Sarriena, s/n, 48940 Leioa, Spain.
[2]Departamento de Física, EPI, Universidad de Oviedo, 33203 Gijón, Spain.
[3]Institute Laue Langevin, 6 rue Jules Horowitz, 38042 Grenoble, France
[4]Instituto de Ciencia de Materiales de Aragón, CSIC–Univ. Zaragoza, 50009 Zaragoza, Spain.
[5]División de Materiales Avanzados, IPCyT, 78216, San Luis Potosí, Mexico.
[6]Departamento de Física de la Materia Condensada, ICMSE-CSIC, Universidad de Sevilla, P.O. Box 1065, 41080 Sevilla, Spain.
[7]Faculty of Humanities and Natural Sciences, Presov University, ul. 17. novembra 1, SK-08116 Presov, Slovakia
[8]Departamento de Física, Universidad de Oviedo, Calvo Sotelo, s/n, 33007 Oviedo, Spain.

*pablo.alvarez@ehu.es

Abstract. Several pseudo-binary $R_xR'_{2-x}Fe_{17}$ alloys (with R = Y, Ce, Pr, Gd and Dy) were synthesized with rhombohedral Th_2Zn_{17}-type crystal structure determined from x-ray and neutron powder diffraction. The choice of compositions was done with the aim of tuning the Curie temperature (T_C) in the 270 ± 20 K temperature range, in order to obtain the maximum magneto-caloric effect around room temperature. The investigated compounds exhibit broad isothermal magnetic entropy changes, $\Delta S_M(T)$, with moderate values of the refrigerant capacity, even though the values of ΔS_M^{Peak} are relatively low compared with those of the R_2Fe_{17} compounds with R = Pr or Nd. The reduction on the ΔS_M^{Peak} is explained in terms of the diminution in the saturation magnetization value. Furthermore, the $\Delta S_M(T)$ curves exhibit a similar caret-like behavior, suggesting that the magneto-caloric effect is mainly governed by the Fe-sublattice. A single master curve for $\Delta S_M/\Delta S_M^{Peak}(T)$ under different values of the magnetic field change are obtained for each compound by rescaling of the temperature axis.

1. Introduction

A wide family of magnetic intermetallic compounds arises from alloying rare-earth (R) elements and 3d transition metals (M) [1,2]. Localized magnetism of rare-earth sublattice combined with an itinerant magnetism of the 3d sublattice makes these magnetic intermetallics very attractive from both fundamental Solid State Physics and commercial applications. In the case of 3d transition metals, stable R-M compounds were obtained for M = Mn, Fe, Co or Ni, where the unpaired 3d electrons of the transition metal component give rise to a net magnetic moment in most cases. The magnetic interactions in R-M compounds comprise, therefore, three different types: the R-R interaction, the R-M interaction and the M-M interaction [3]. The R-R interaction is the weakest due to the localized character of the electrons.

The Fe-rich R_2Fe_{17} intermetallics have attracted a renewed interest as promising materials for room temperature magnetic refrigeration technology due to a remarkable magneto-caloric effect. For R = Pr or Nd moderate values for the maximum of the isothermal magnetic entropy change, ($\Delta S_M^{Peak} \approx 6$ J/kg K^{-1} for a change of the applied magnetic field $\mu_0\Delta H = 5$ T), together with broad maxima of the $\Delta S_M(T)$ curves, give rise to a large refrigerant capacity (*RC*) [4-6]. In addition, the coexistence of both direct and inverse magneto-caloric effect has been recently discovered in Er_2Fe_{17} compound, which also exhibits large magneto-volume anomalies [7]. From the structural point of view, these compounds present polymorphism with two different types of crystal structure depending on the rare-earth element. From Ce to Sm the R_2Fe_{17} compounds crystallize in the rhombohedral Th_2Zn_{17}-type ($R\overline{3}m$ space group), with the rare earth occupying a unique crystallographic site, 6c (in Wychoff notation [8]), whereas the Fe atoms occupy four non-equivalent positions: 6c, 9d, 18f and 18h [6,9]. In turns, the crystal structure is hexagonal (Th_2Ni_{17}-type, $P6_3/mmc$ space group) for the alloys with R = Dy to Lu. In the latter case, the rare earth occupies two different sites: 2b and 2d, characterized by a rather similar local atomic arrangement of Fe next-neighbour atoms and by a slight different arrangement of the rare-earth atoms. The Fe atoms also occupy four different crystallographic sites: 4f, 6g, 12j and 12e [1,7,10]. Both crystal structures are found for R = Gd and Tb. Moreover, the mixing of two different rare-earth elements in the form $R_xR'_{2-x}Fe_{17}$ can result in a single-phase compound, depending on the R_2Fe_{17} and R'_2Fe_{17} crystal structures [11,12]. Therefore, the combination of two R elements can facilitate the synthesis of single-phase materials with one of the two possible crystal structures, which is sometimes difficult. In this way, it is also feasible to modify the Curie temperature (T_C) of R_2Fe_{17} intermetallics by mixing different rare earth elements [13,14].

In the present work we report on the synthesis, the crystal structure, the magnetic properties and the magneto-caloric response of five pseudo-binary intermetallic alloys: $Y_{1.2}Ce_{0.8}Fe_{17}$, $Pr_{1.5}Ce_{0.5}Fe_{17}$, $Gd_{1.3}Ce_{0.7}Fe_{17}$, $Dy_{1.15}Ce_{0.85}Fe_{17}$ and $YPrFe_{17}$. Such compositions were selected with two main goals: the possibility of tuning the value of the Curie temperature in the immediacy of room temperature and also, how the changes in the R-sublattice could affect the magneto-caloric effect.

2. Experimental

The starting materials for the preparation of as-cast pellets (Goodfellow, 99.9% pure rare earth elements relative to rare earth content and 99.99% Fe pieces) were mixed in the nominal molar ratio 2:17. The polycrystalline ingots were arc melted under Ar atmosphere. Each specimen was wrapped in tantalum foil and sealed under vacuum in a quartz ampoule, and further annealed at 1263 K for 7 or 12 days to ensure their homogeneity, followed by water-quenching. Energy dispersive x-ray spectroscopy (EDS) confirmed the nominal composition of the alloys.

Crystal structure and lattice parameters were studied by means of both x-ray (XRD) and neutron powder diffraction (ND). XRD studies were performed at room temperature in a high resolution powder diffractometer (Seifert model XRD3000) operating in Bragg-Brentano geometry using Cu $K\alpha$ radiation ($\lambda = 1.542$ Å), with scans in 2θ registered between 2° and 130° with $\Delta 2\theta = 0.025°$ steps and counting times of 20 s per point. ND patterns were collected on the D1B high-flux two-axis powder diffractometer ($\lambda = 2.52$ Å) at $T = 300$ K, at the ILL (Grenoble, France). The full-profile analysis of the diffraction patterns was carried out with the FullProf suite package [15]. Peak broadening contributions originated from small crystals and/or microstrain effects [16] were not observed.

Magnetization measurements were carried out in a Quantum Design SQUID and a Lakeshore VSM model 7407 magnetometers. The temperature dependence of the magnetization, $M(T)$, under a low applied magnetic field ($\mu_0H = 5$ mT) was measured in order to estimate the T_C value of the samples as the minimum of the dM/dT vs. T curve. Isothermal magnetization vs. applied magnetic field curves, $M(H)$, were measured in the temperature range 90 - 390 K. For each $M(H)$ curve the applied magnetic field was increased from 0 up to 1.5 T. The isothermal magnetic entropy variation, $\Delta S_M(T,H)$, due to a change of the applied magnetic field from an initial value $H = 0$ to a final value H is calculated using the Maxwell relation:

$$\Delta S_M(T,H) = \int_0^H \left(\frac{\partial M(T',H')}{\partial T'} \right)_{T'=T} dH' \tag{1}$$

3. Results and Discussion

Figure 1 depicts the XRD (a) and the ND (b) pattern of $Gd_{1.3}Ce_{0.7}Fe_{17}$ and $Dy_{1.15}Ce_{0.85}Fe_{17}$ alloys, respectively. The other three samples show similar powder diffraction patterns. The observed intensity peaks of the XRD and ND patterns can be indexed as the Bragg reflections corresponding to the rhombohedral Th_2Zn_{17}-type crystal structure with $R\bar{3}m$ space group (#164). There is not any trace of the hexagonal Th_2Zn_{17}-type phase in the diffraction patterns. The main crystallographic information is given in Table 1. From the fit of the diffraction patterns it was evidenced that the R and R' atoms share the 6c site with the same atomic coordinates. Hence, mixing Ce with Y and Gd, as well as Pr with Y stabilizes the rhombohedral phase versus the hexagonal one for the Y_2Fe_{17}, Gd_2Fe_{17} and Dy_2Fe_{17} binary intermetallic compounds. It should be noticed that the Pr containing compounds have the largest cell volume of the studied pseudobinary compounds, as a consequence of the lanthanide contraction. Additionally, a small amount (< 3%) of α-Fe impurity phase ($Im\bar{3}m$ space group) was found in all the compounds, similarly as that occurring in the rhombohedral R_2Fe_{17} binary compounds. The ratio c/a ~ 1.45 is in good agreement with those reported for the rhombohedral R_2Fe_{17} alloys [6,9].
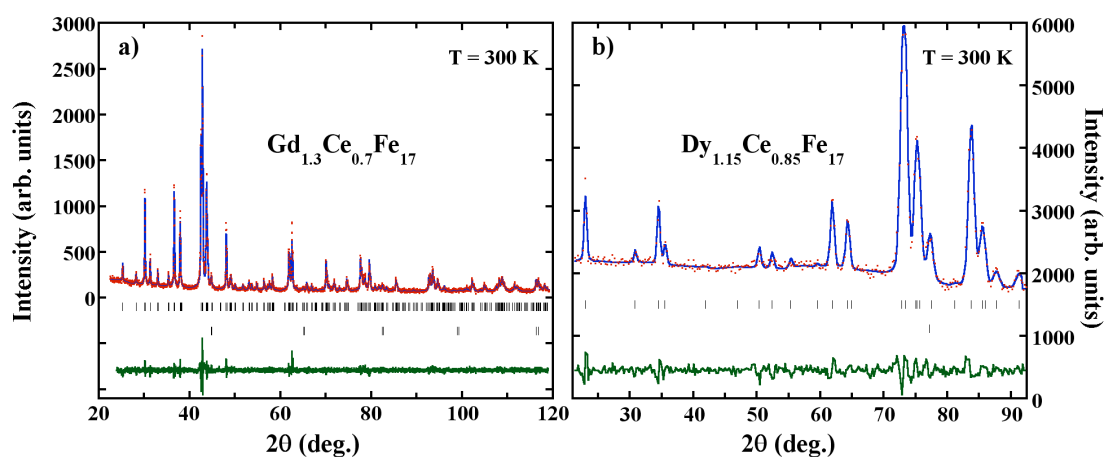

Figure 1. Observed (dots) and calculated (solid line) a) x-ray and b) neutron diffraction patterns collected at T = 300 K for $Gd_{1.3}Ce_{0.7}Fe_{17}$ and $Dy_{1.15}Ce_{0.85}Fe_{17}$, respectively. Vertical bars represent the positions of the Bragg reflections; the first row corresponds to the Th_2Zn_{17}-type crystal structure nuclear scattering, whereas the second row corresponds to the α-Fe impurity phase. The observed–calculated difference is depicted at the bottom of each figure.

The Curie temperatures of $Y_{1.2}Ce_{0.8}Fe_{17}$ (253 ± 5 K), $Pr_{1.5}Ce_{0.5}Fe_{17}$ (264 ± 5 K), $Gd_{1.3}Ce_{0.7}Fe_{17}$ (293 ± 5 K), $Dy_{1.15}Ce_{0.85}Fe_{17}$ (273 ± 5 K) and $YPrFe_{17}$ (290 ± 5 K), are in between those reported values for Y_2Fe_{17} (310 ± 4 K) [17], Ce_2Fe_{17} (Néel temperature = 210 K) [18], Pr_2Fe_{17} (286 ± 2 K) [9], Gd_2Fe_{17} (476 K) [19] and Dy_2Fe_{17} (370 K) [20]. Mixing different R ions gives rise to variations in the Fe–Fe next neighbor distances along the c-axis, which strongly affects the magnetic interactions, and thus modifies the value of T_C [7,9]. Therefore, the Curie temperature of the resulting pseudo-binary alloys can be tuned between those values of the pure binary compounds.

The saturation magnetization, M_S, at T = 85 K (see Table 2) was estimated from the fit of the magnetic field dependence of the magnetization to an approach-to-saturation law [21],

$$M = M_S\left(1 - \frac{b}{H^2}\right) + \chi_0 H \qquad (2)$$

These results can be understood if it is assumed that the magnetic structure is that of the parent R_2Fe_{17} alloys. The Pr-containing alloys show higher M_S values due to the collinear ferromagnetic structure of Pr_2Fe_{17}. In this sense, $YPrFe_{17}$ and $Pr_{1.5}Ce_{0.5}Fe_{17}$ have similar M_S values, because Y has no magnetic moment and, even though the pure Ce_2Fe_{17} has a complicated magnetic phase diagram, the Cerium ion has a weak magnetic moment [22,23] and its contribution to the total magnetization of the alloy can be neglected. The $Y_{1.2}Ce_{0.8}Fe_{17}$ has an intermediate value because only the Fe-sublattice contributes to the M_S. The antiparallel coupling between the Dy^{+3} and Gd^{3+} magnetic moments and those of the Fe sublattice explains the lower M_S value exhibited by the $Gd_{1.3}Ce_{0.7}Fe_{17}$ and $Dy_{1.15}Ce_{0.85}Fe_{17}$.

TABLE 1. Cell parameters and atomic positions corresponding to the studied compounds (with rhombohedral crystal structure) obtained from room temperature XRD patterns.

	$Y_{1.2}Ce_{0.8}Fe_{17}$	$Pr_{1.5}Ce_{0.5}Fe_{17}$	$Gd_{1.3}Ce_{0.7}Fe_{17}$	$Dy_{1.15}Ce_{0.85}Fe_{17}$	$YPrFe_{17}$
a (Å)	8.490 (1)	8.565 (1)	8.523 (1)	8.487 (1)	8.540 (1)
c (Å)	12.394 (1)	12.487 (2)	12.436 (1)	12.417 (3)	12.419 (1)
c/a	1.460	1.455	1.459	1.461	1.454
V (Å^3)	774.1 (1)	790.2 (2)	782.2 (1)	773.1 (2)	784.3 (2)
R-6c: z	0.340 (1)	0.320 (1)	0.344 (1)	0.359 (2)	0.348 (3)
Fe-6c: z	0.098 (2)	0.091 (2)	0.096 (1)	0.125 (6)	0.092 (1)
Fe-18f :x	0.281 (1)	0.287 (3)	0.292 (2)	0.291 (2)	0.293 (1)
Fe-18h: x	0.165 (1)	0.172 (1)	0.168 (1)	0.160 (2)	0.169 (2)
Fe-18h: z	0.481 (2)	0.481 (2)	0.490 (1)	0.482 (2)	0.489 (1)
R_B	11.0	10.8	4.5	5.7	5.7
χ^2 (%)	1.5	3.0	1.4	1.2	1.5

According to the saturation magnetization, the Pr-based pseudo-binary intermetallics would exhibit the largest magnetic entropy change because of their higher saturation magnetization values. The isothermal magnetic entropy change, ΔS_M, was calculated from the set of isothermal magnetization vs. applied magnetic field, $M(H)$, curves. In figure 2 those $M(H)$ curves corresponding to the $Gd_{1.7}Ce_{0.3}Fe_{17}$ alloy measured between 220 and 390 K with a temperature step of 10 K are shown.
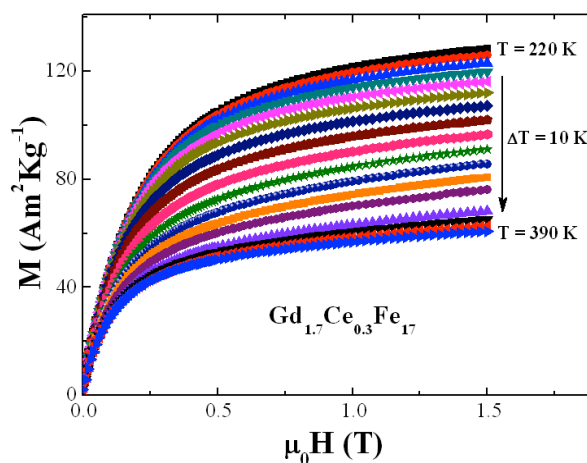

Figure 2. Magnetic field dependence of the isothermal magnetization for $Gd_{1.7}Ce_{0.3}Fe_{17}$.

The Pr-containing pseudo-binary alloys have the largest peak values of the magnetic entropy change (see figure 3), $|\Delta S_M|^{Peak}$, as expected from the relative M_S values. Besides that, the $|\Delta S_M|(T)$ curves are broad, being the full width at half maximum, δT_{FWHM}, over 80 K for $\mu_0 \Delta H = 1.5$ T. This is an important parameter to be taken into account when the refrigerant capacity (RC) of a material with potential interest in magnetic refrigeration has to be evaluated [5]. This figure of merit can be estimated as the product of the full width at half maximum and the peak value. The field dependence of the refrigerant capacity was also obtained (see inset in figure 3). The values for $Y_{1.2}Ce_{0.8}Fe_{17}$, $Pr_{1.5}Ce_{0.5}Fe_{17}$ and $YPrFe_{17}$ are lower than those of the parent Pr_2Fe_{17} and Y_2Fe_{17} alloys [24], as a direct consequence of the reduction of M_S. However, Ce_2Fe_{17} presents an antiferromagnetic to paramagnetic phase transition, which has low refrigerant capacity [25]. $Dy_{1.15}Ce_{0.85}Fe_{17}$ has increased its RC with respect to the pure Dy_2Fe_{17} alloy [25]. As far as we know, no data of Gd_2Fe_{17} was published yet. Even though $|\Delta S_M|^{Peak}$ of the studied compounds is much lower than that of the polycrystalline Gd, the RC reaches 65% of RC_{Gd}.

TABLE 2. Magnetic and magneto-caloric properties ($\mu_0 \Delta H = 1.5$ T) of the pseudobinary alloys.

	$Y_{1.2}Ce_{0.8}Fe_{17}$	$Pr_{1.5}Ce_{0.5}Fe_{17}$	$Gd_{1.3}Ce_{0.7}Fe_{17}$	$Dy_{1.15}Ce_{0.85}Fe_{17}$	$YPrFe_{17}$	Pure Gd
T_C (K)	253(5)	264(5)	293(5)	273(5)	290(5)	289(5)
M_S (A m^2 kg^{-1})	113	135	87	88	134	-
$|\Delta S_M^{Peak}|$ (J K^{-1} kg^{-1})	1.6	2.4	0.8	1.3	2.3	4.3
RC (J kg^{-1})	92	103	83	83	98	160
δT_{FWHM} (K)	57	42	107	65	43	37

It was shown, both theoretically and from a phenomenological approach, that there exists a master curve for the magnetic entropy change in magnetic materials with a second-order phase transition [26-28]. This master curve implies the collapse of the properly rescaled $\Delta S_M(T)$ curves for different values of the applied magnetic field change, and consequently it could be useful to predict the magnetic field and temperature dependences of ΔS_M in those materials which do not follow a mean field approach [29].
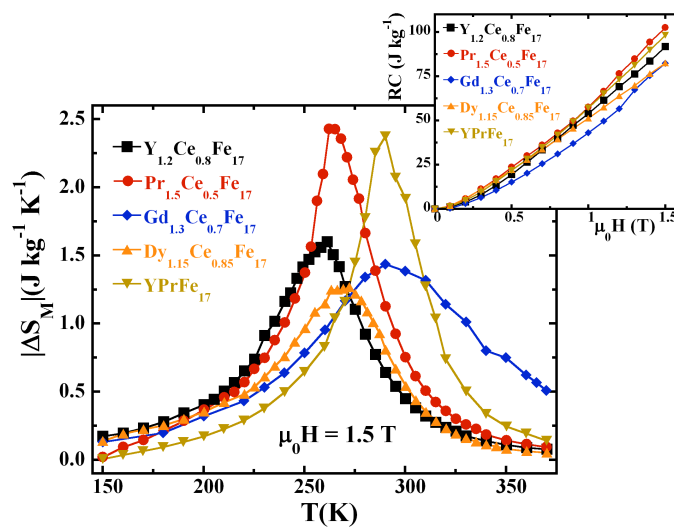

Figure 3. Temperature dependence of the magnetic entropy change for $R_xR'_{2-x}Fe_{17}$ alloys under $\mu_0 \Delta H = 1.5$ T. Inset shows the field dependence of refrigerant capacity.

Therefore, this allows the extrapolation of the $|\Delta S_M(T)|$ curves for different values of the applied magnetic field change, as well as for the estimation of $|\Delta S_M(T)|$ curves in other intermetallic compounds with related compositions, in which the rare earth metal and/or the relative amount is varied. It is theoretically derived from the knowledge of the magnetic equation of state, whereas, in a phenomenological way, it is obtained from the $\Delta S_M(T)$ curves themselves. We will focus in the phenomenological procedure. Firstly, each $\Delta S_M(T)$ curve is normalized to the value of the corresponding ΔS_M^{Peak}. Secondly, the temperature axis is rescaled imposing that a reference point in the $\Delta S_M(T)$ curve corresponding to a previously selected fraction of ΔS_M^{Peak}, makes the rescaled temperature, θ, to be equal 1 ($\theta = -1$) when the temperature at which the reference point, T_r, is chosen is $T_r > T_C$ ($T_r < T_C$) in the following way [30] $\theta = (T - T_C)/(T_r - T_C)$ [(or in the case of $T_r < T_C$, $\theta = -(T - T_C)/(T_r - T_C)$]. This procedure has been successfully tested in several metallic glasses as well as in polycrystalline magnetic solids [28,31]. However, if a secondary magnetic phase is present in the material, the temperature axis is rescaled in the form [30]:

$$\theta = -(T - T_C)/(T_{r1} - T_C) \qquad \text{for } T < T_C$$

$$\theta = (T - T_C)/(T_{r2} - T_C) \qquad \text{for } T > T_C \qquad (3),$$

where T_{r1} and T_{r2} are the temperatures, below and above T_C respectively, corresponding to the two reference points for each curve that correspond to $a \times \Delta S_M^{Peak}$ (with a in between 0 and 1). In this work a was selected to be 0.5. For this value, the reference points correspond to the half maximum of the $\Delta S_M(T)$ curves. The phenomenological $\Delta S_M(T)\backslash \Delta S_M^{Peak}$ curves were obtained using two reference temperatures. These curves for different magnetic fields collapse into the same curve for each sample in the paramagnetic zone (see figure 4 for the GdCeFe alloy). However, there are slight differences when comparing these master curves for all the alloys at the maximum magnetic field change (see the inset in figure 4).
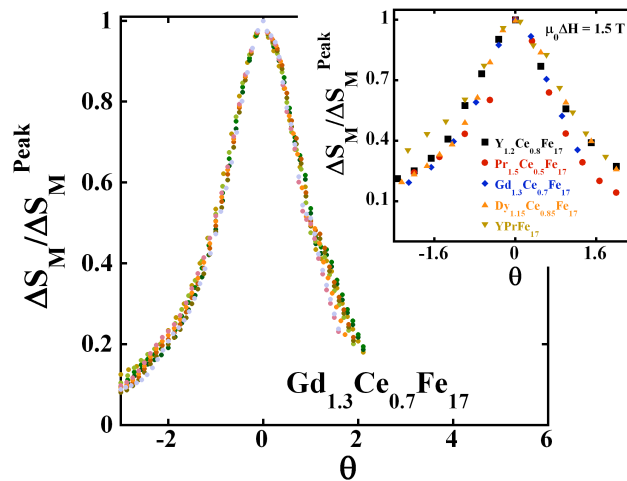

Figure 4. Master curve for $Gd_{1.3}Ce_{0.7}Fe_{17}$ obtained using two temperatures of reference (see text for details). The inset shows a comparison of the master curves for the studied pseudo-binary alloys under a magnetic field change $\mu_0\Delta H = 1.5$ T.

Conclusions

Room temperature x-ray and neutron powder diffraction confirm that the crystal structure of the $Y_{1.2}Ce_{0.8}Fe_{17}$, $Pr_{1.5}Ce_{0.5}Fe_{17}$, $Gd_{1.3}Ce_{0.7}Fe_{17}$, $Dy_{1.15}Ce_{0.85}Fe_{17}$ and $YPrFe_{17}$ pseudo-binary intermetallic compounds is rhombohedral with a space group $R\overline{3}m$. The values of the Curie temperature can be tuned between 250 and 295 K by small changes in the composition. In this way, it is possible to select the temperature of the maximum of $|\Delta S_M(T)|$. The Pr-containing compounds exhibit the higher maximum magnetic entropy change, as they have the largest saturation magnetization due to the collinear parallel configuration of both Fe and Pr sublattice magnetic moments. In addition, the calculated values for the RC can reach 65% of that for pure Gd.

Acknowledgments

References

[1]   Buschow K H J 1977 *Rep. Prog. Phys.* **40** 1179.
[2]   Brouha M *et al.* 1974 *IEEE Trans. Mag.* **10** 182.
[3]   Piqué C *et al.* 2007 *Phys. Rev. B* **75** 224424.
[4]   Mandal K *et al.* 2004 *J. Phys. D: Appl. Phys.* **37** 2628.
[5]   Gorria P *et al.* 2008 *J. Phys. D: Appl. Phys.* **41** 192003.
[6]   Álvarez P *et al.* 2010 *J. Phys.: Condens. Matter* **22** 216005.
[7]   Álvarez P *et al.* 2012 *Phys. Rev. B* **86** 184411.
[8]   *International Tables for Crystallography* 2005, ed T Hahn (IUCr, Springer, Dordrecht, The Netherlands).
[9]   Gorria P *et al.* 2009 *Acta Mater.* **57** 1724.
[10]   Tereshina I *et al.* 2005 *J. Alloys Compd.* **404** 172.
[11]   Xiao Y G *et al.* 2006 *J. Alloys Compd.* **407** 1.
[12]   Xiao Y G *et al.* 2006 *J. Alloys Compd.* **419** 15.
[13]   Ben Kraiem M S *et al.* 2003 *J. Magn. Magn. Mater.* **256** 262.
[14]   Richomme M S *et al.* 2010 *J. Alloys Compd.* **494** 5.
[15]   Rodríguez Carvajal J 1993 *Physica B* **192** 55.
[16]   Martinez-Blanco D *et al.* 2008 *J. Phys: Condens. Matter* **20** 335213.
[17]   Arnold Z *et al.* 1994 *IEEE Trans. Mag.* **30** 619.
[18]   Fujii H *et al.* 1995 *J. Alloys Compd.* **219** 10.
[19]   Shen B G *et al.* 1998 *J. Phys. D: Appl. Phys.* **31** 2438.
[20]   Wang J L *et al.* 2007 *Phys. Rev. B* **75** 174423.
[21]   Cullity B D 1972, *Introduction to Magnetic Materials* (Addison-Wesley, Reading, MA).
[22]   Isnard O *et al.* 1997 *J. Alloys Compd.* **262** 198.
[23]   Grandjean F *et al.* 1999 *Solid State Comm.* **109** 779.
[24]   Álvarez P *et al.* 2011 *Mat. Chem. Phys.* **131** 18.
[25]   Álvarez Alonso P 2011, *Magnetocaloric and magnetovolume effects in Fe-based alloys*, PhD Thesis, (University of Oviedo, Oviedo , Spain).
[26]   Franco V *et al.* 2006 *Appl. Phys. Lett.* **89** 222512.
[27]   Álvarez P *et al.* 2011 *Intermetallics* **19** 982.
[28]   Franco V *et al.* 2007 *Europhys. Lett.* **79** 47009.
[29]   Franco V and Conde A 2010 *Int. J. Refrig.* **33** 465
[30]   Franco V *et al.* 2009 *J. Magn. Magn. Mater.* **321** 1115.
[31]   Álvarez P *et al.* 2010 *J. Alloys Compd.* **504S** S150.